Passive Mooring-based Turbine Repositioning Technique for Wake Steering in Floating Offshore Wind Farms

Journal of Physics: Conference Series **2767** (2024) 092056 doi:10.1088/1742-6596/2767/9/092056

Passive Mooring-based Turbine Repositioning Technique for Wake Steering in Floating Offshore Wind Farms

Yuksel R. Alkarem[1], Kimberly Huguenard[1], Amrit S. Verma[2], Diederik van Binsbergen[3], Erin Bachynski-Polić[3], Amir R. Nejad[3]

[1]Civil and Environmental Engineering Department, University of Maine, 35 Flagstaff Road, Orono, Maine 04469, USA

[2]Mechanical Engineering Department, University of Maine, 35 Flagstaff Road, Orono, Maine 04469, USA

[3]Department of Marine Technology, Norwegian University of Science and Technology (NTNU), Jonsvannsveien 82, 7050 Trondheim, Norway

E-mail: yuksel.alkarem@maine.edu

Abstract. Power loss due to wake effects from upstream wind turbines is an important factor in the design of floating wind farms. These wake disturbances also increase fatigue loads on downstream units. Economic-driven wind farm layout optimization may culminate in non-standard, irregular configurations of offshore wind farms that deviate from conventional engineering practices. Consequently, wind farm developers are inclined towards a more geometrically coherent layout that are sub-optimal. Floating wind turbines horizontal offsets can be used to overcome wake losses. In this study, a novel method suggesting various mooring orientation methods to passively reposition the wind turbines in the farm to maximize annual energy yield. Preliminary parametric optimization demonstrates the effectiveness of the proposed method for standard floating wind farm designs to reduce wake effects by as much as 30% at rated wind speed compared to a baseline case, while preserving the farm's overall uniformity.

1. Introduction

Recent develpments in offshore wind technologies have focused on reducing costs and enhancing their effeciency. As wind farms move towards deep waters [1], floating wind projects are growing and more seabed leasing in deep waters will take place worldwide [2].

An important aspect in the design of offshore wind farms (OWF) is the annual energy production (AEP) [3]. After selecting a site, the first step to optimize the AEP is by assessing the optimal selection of each individual wind turbine (WT) location in the farm to mitigate wake effects. The wake effects are exacerbated further the more the OWF is composed of clusters of turbines. The optimal arrangement can be either symmetrical or irregular. Researches have shown that symmetrically optimal configuration can be achieved with farm-level parametric variation [4].

Even though stochastic arrangements tend to increase AEP, highly irregular arrangements are practically difficult to implement and standardize. Therefore, the developer tends to design OWFs with uniformly distributed WTs due to reasons such as visual impact restrictions, reduced

maximum turbine loads due to turbulence (as spacing between WT tend to be larger for symmetrical layouts [4]), or other factors imposed in certain locations. For example, New England wind energy lease areas [5] require clearly delineated transit corridors, navigational safety, and ease of search and rescue operations near or inside the farm [6].

A well documented approach to combat wake losses is wind farm control. The strategy is implemented on the individual WTs to achieve an optimum wind-farm objective [7]. One example of such systems is the misaligned yaw-based wake redirection approach [8] that depends on active controls that sacrifice upstream turbine power to steer the downstream wake. However, this requires control effort and derates upstream turbines.

Floating wind turbines (FWTs) are implemented when the water depth exceeds a certain threshold (around 60m) where a fixed substructure is no longer feasible. The key advantage of FWTs is that they can operate in areas with more consistent and faster winds, resulting in higher capacity factors of the floating wind farm (FWF) compared to their fixed-bottom counterparts as demonstrated by many projects around the world such as the Hywind Scotland pilot project [9]. Certainly, wake mitigation approaches for onshore or fixed-bottom offshore WTs can also be implemented on FWTs. However, due to the rigid-body motion allowed by the floating platform, the dynamics of the system are altered. The mobility of FWTs can either deter the wind farm control such as the case with yaw and induction-based turbine repositioning (YITuR) [10] or can be used to mitigate the wake effects even further by the turbine repositioning (TR) in real-time to mitigate wake effects [10, 11, 12, 13]. Figure 1(a & b) demonstrates the wake effects on FWF systems. The literature illustrates the effectiveness of integrating TR technique with active yaw-based wake redirection strategies to dynamically maximize energy yield [14, 15].

A FWT's horizontal excursion is governed by the station-keeping system (typically mooring lines). The mooring configuration determines the dynamic behavior of the floater under the combination of various environmental forcing. The stiffer the system due to mooring configuration the shorter the natural period of the system and the more the system's offset is constricted and vice versa. Therefore, it is of importance to consider macro-scale parameters at the farm level during mooring design and explore their potential to mitigate losses due to wake effects. Researchers have explored active mooring system controls for TR for wake mitigation [16] while others have demonstrated that the passive relocation of WTs, by the static variation of mooring lines, can boost wind farm efficiency [17, 18]. However, such optimal strategies may lead to highly irregular and hard-to-maintain mooring setups. Characterizing a distinct set of mooring-related parameters for each turbine can present significant logistical difficulties within the context of supply chain management.

This paper proposes a TR technique for layout economics (TRTLE) through farm-level mooring reconfiguration as illustrated in Figure 1(c). The proposed solution is constrained to prevent turbines collision. Such limitations are discussed by Ref. [15] when they observed movable ranges of the turbines overlap. Another issue is the power cable (also called umbilical). It must be designed specifically to prevent high tensions and curvatures that come along with high offsets. The design of suspended umbilical for FWT application in deep water is investigated by Ref. [19], and an approach to the dynamic inter-array cable optimal design with a lazy-wave configuration is provided by Ref. [20]. Extreme static and dynamic responses of the umbilical in very deep waters must be considered [21]. Sufficient spacing under failure conditions is ensured and the umbilical is designed to accommodate high excursions.

The remaining structure of this paper proceeds as follows: Section 2 gives a general background on the methodology as well as the scope and limitations. Section 3 presents a brief description of the problem and of the parametric study and optimization procedure. Results regarding parametric analysis and umbilical design are provided in Section 4, while Section 5 concludes with remarks on how to proceed with future studies.

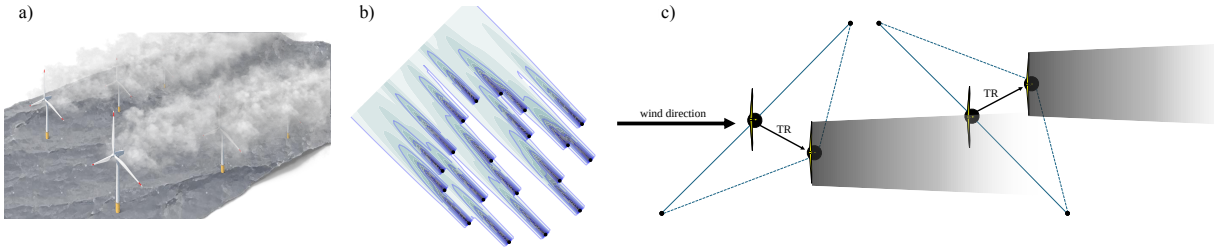

Figure 1. a) illustration of FWF and wake effects caused by upstream turbines, b) top view highlighting velocity deficit in the wakes and c) the proposed TRTLE technique utilizing floater displacement from the mooring design to avoid wake from upstream turbines (repositioning shown is not to scale).

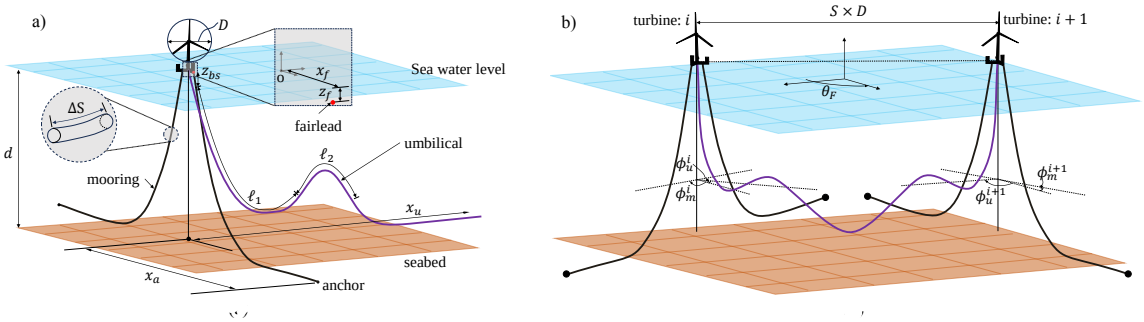

Figure 2. a) illustration of stand-alone turbine parameters and b) farm level parameters.

2. Methodology

The problem is characterized by parameters of four categories: farm, environmental, mooring, and umbilical. Each parameter is further classified into sub-categories depending on whether it varies in an intra-array (IA) fashion (IA-variable) or not (IA-fixed) as summarized and illustrated in Table 1 and Figure 2. The farm-level parameters determine the number of turbines to be placed at the site. The main driving parameter for the mooring design is the catenary coefficient, β. For a mooring line of length, L_m, the catenary coefficient ranges between zero and one and can be described as

$$\beta = \frac{L_m - L_{m_{\min}}}{L_{m_{\max}} - L_{m_{\min}}}, \tag{1}$$

where $L_{m_{\min}}$ and $L_{m_{\max}}$ are the minimum and maximum lengths of the mooring cable, respectively;

$$\begin{aligned} L_{m_{\min}} &= \sqrt{(z_f - z_a)^2 + (x_f - x_a)^2} \\ L_{m_{\max}} &= (z_f - z_a) + (x_f - x_a). \end{aligned} \tag{2}$$

2.1. Hydrodynamic and mooring model:

The model used for the floating platform, the mooring, and power cable is Orcina OrcaFlex driven via a dynamic link library (DLL) through the python OrcFxAPI interface. This allows optimization processes and parametric analyses to be conducted effortlessly while enabling coupling with the wake model. The turbine model is the UMaine VolturnUS-S reference platform [22] supporting the IEA 15-megawatt (MW) offshore reference wind turbine [23].

Table 1. parametric description of the problem

Category	parameter	symbol	sub-category
farm	layout orientation	θ_F	IA-fixed
	spacing ratio	S	IA-fixed
environmental	water depth	d	IA-fixed
mooring	number of mooring lines	N_m	IA-fixed
	fairlead horizontal distance	x_f	IA-fixed
	fairlead vertical distance	z_f	IA-fixed
	anchor horizontal distance	x_a	IA-fixed
	catenary coefficient	β	IA-fixed
	mooring segment length	ΔS	IA-fixed
	mooring orientation	ϕ_m	IA-variable
umbilical	umbilical orientation	ϕ_u	IA-variable
	bend stiffener range	z_{bs}	IA-fixed
	umbilical horizontal reach	x_u	IA-fixed
	umbilical sectional lengths	ℓ_1, ℓ_2	IA-fixed

2.2. Wake model:
The wake is simulated via the open-source FLOw Redirection and Inductive in Steady State (FLORIS v3.0.0) software developed by the National Renewable Energy Laboratory (NREL) and Delft University of Technology. The wake deflection and velocity models are configured as Gaussian and the combination model is the sum of squares freestream superposition model (SOSFS) [25]. A fixed turbulence intensity of $I_\infty = 6\%$ is assumed with wake expansion coefficients $k_a = 0.10$, $k_b = 0.004$, transition point near-far wake coefficients $\alpha_w = 0.58$, $\beta_w = 0.077$, and no lateral wake deflection [26].

2.3. Scope of study and key assumptions
The investigation in this research is restricted to a singular site shape but can be easily extended to more complex site boundaries. Additionally, this study only scrutinizes the effectiveness of the proposed approach from the steady state perspective. In future work, the dynamic properties of the system will be studied. This study only focuses on deep water applications. The water depth is fixed at $d = 1000$m and the mooring type is the same chain properties described in the definition of the VolturnUS-S. These properties might not be realistic for this preliminary study. Future research aims to bridge these gaps by applying parametric study to investigate water depth variation and synthetic mooring type application. Some key assumptions are 1) the seabed slope is set to zero and bathymetric variations are not included in this study, 2) the main driving force of the turbine's repositioning is the thrust force applied at the hub height, 3) wind speed across the wind rose is constant and is equal to the rated wind speed, and 4) wave and current actions are not included in this study.

3. Problem analysis, and optimization schemes
3.1. Analysis flowchart
The flowchart in Figure 3 provides a brief description of the process conducted in this study. The site boundaries are provided as input to the algorithm and the turbine locations inside the boundaries are created based on the layout orientation θ_F and a given spacing ratio, $S = x/D$

between the turbines, where x is the horizontal distance between two neighboring turbines in either directions and D is the rotor diameter of the turbine. The site in this study is arbitrarily selected as a square. The AEP for the baseline case can be computed given a turbine model and the energy resources at the site. The wind rose is selected from the case study given by the international energy agency (IEA) Task 37 [27] with dominant wind direction from the west. As for TRTLE analysis, the IA-fixed properties are used to determine the catenary configuration of the mooring lines under two constraints: maximum excursion and maximum allowable horizontal anchor spread. These two constraints address limited excursion due to the umbilical connection and ensure turbines do not collide with each other in case of a mooring line failure.

The constraints are met via running an optimization problem through varying β until excursion limits are met. An excursion error threshold of 5m is set. The framework used for optimization is the open-source Optuna package [28] using a Tree-structured Parzen Estimator (TPE) Sampler algorithm [29]. The ratio of maximum platform offset to water depth, e_{max}/d, is selected to be between 0.3 and 0.4. This ratio is chosen to demonstrate the potential of the proposed design. The recommended practice in the literature for excursion to water depth ratio is between 0.125 to 0.3 [30]. However, ratios up to 0.5 are reported in the literature [31]. Anchor horizontal spread is limited to half the spacing between the turbines, $x_a = \frac{S \times D}{2}$.

To achieve fast computation, the platform excursion of the stand-alone turbine in the horizontal plane as a function of wind speed and direction is computed with a radial discretization value of $\Delta\theta = 22.5°$. The generated excursion amplitude is identical for all turbines since they share the same IA-fixed parameters. An example of excursion values as functions of wind speed, u, and direction, θ is illustrated in Figure 4(a).

The optimization process begins via adjusting the IA-variables, dictating how the line headings are oriented in the farm (to be discussed in section 3.2). Once IA-variables are selected, the algorithm loops over all wind speeds and wind directions. For each case, the flow field is first computed to obtain thrust forces on all turbines. Subsequently, the platform excursion is quantified and the turbines are relocated. Since the new turbine locations have different wind velocities, a recursive loop takes place to find the flow field, relocating the turbines until their locations converge. The average location of all turbines must meet a relocation tolerance of 0.25m (a fraction of the mean offset values). The method requires the system to reach a new equilibrium in all degrees of freedom of the rigid body motion. Then, energy is computed for the given wind speed and wind direction and the AEP is computed given the wind speed/direction frequencies.

3.2. Mooring orientation methods

Preliminary analyses suggest a linear mooring arrangement (2-line configuration in opposing directions) achieves high difference between the static equilibrium position and the excursion caused by the thrust force. On the farm-level, two methods for mooring orientation are presented: 1) the chessboard-pattern, creating a zigzag mooring orientation throughout the farm, and 2) plane variation, altering mooring orientation linearly in the $x - y$ plane. Plan views of these orientation methods are shown in Figure 4(b).

4. Results

4.1. Parametric analysis

To investigate TRTLE's impact on farm performance relative to the baseline (defined here as turbines having identical mooring orientation with equal offsets or equivalently zero offset), a parametric analysis is conducted. Key variables included farm orientation, $\theta_F \in [0°, 45°]$ at 5° intervals, and turbine spacing ratio, $S \in [6, 10]$ in increments of 0.5. The layout constraints included a 15km square boundary without turbine quantity limitations, subject to the spacing constraint.

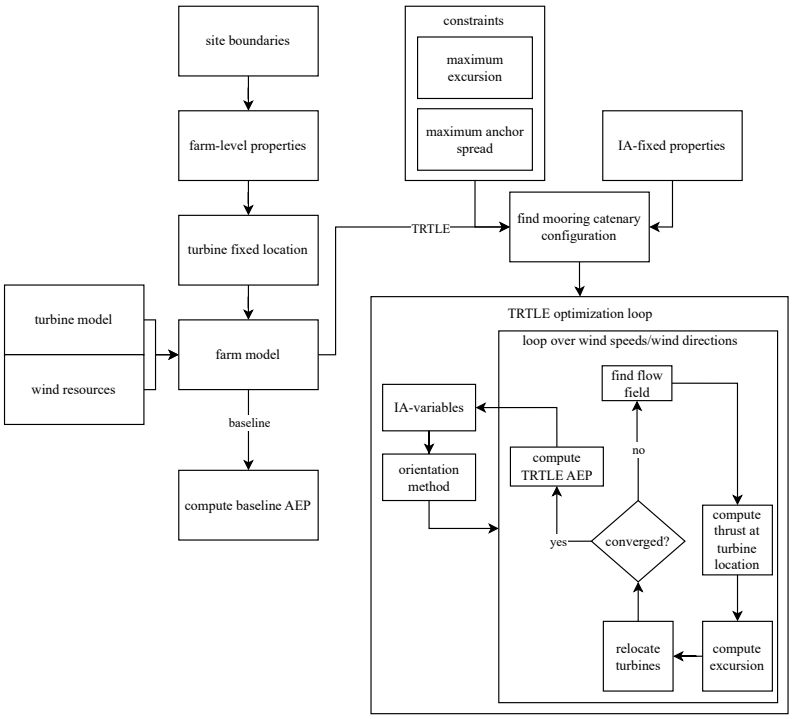

Figure 3. Flowchart for the computation of AEP for the baseline and TRTLE cases.

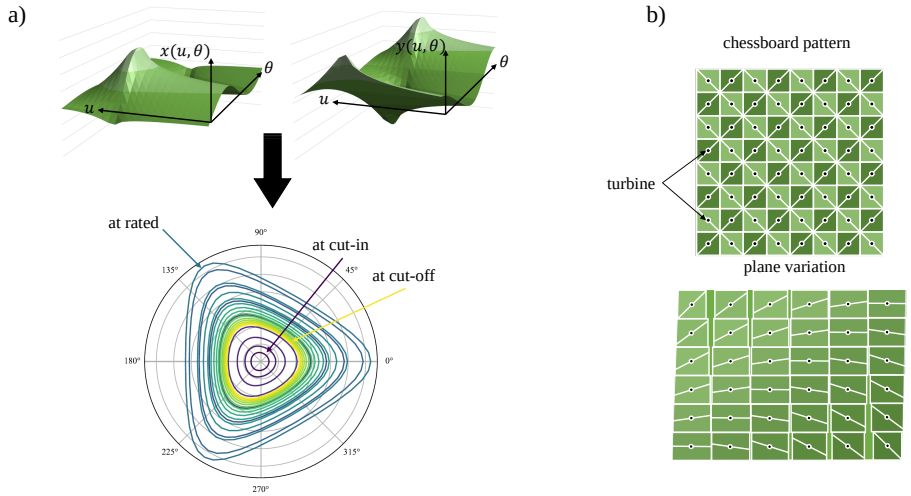

Figure 4. a) platform excursion functions example based on wind speed and direction, b) various orientation methods used in farm-level optimization, with red lines showing mooring line orientation and black dots marking turbine locations.

Subsequently, the TRTLE optimization is executed, proposing various mooring orientation methods to maximize AEP. A consistent trial count of 500 is maintained for all configurations, a number deemed sufficient for optimizer convergence based on preliminary sensitivity trials (data not presented). Parametric analysis is depicted in Figure 5, highlighting wake loss avoidance within the farm when using TRTLE relative to the baseline. Notably, power output enhancement is achieved across-the-board. The extent of this enhancement varies relative to the extremity of

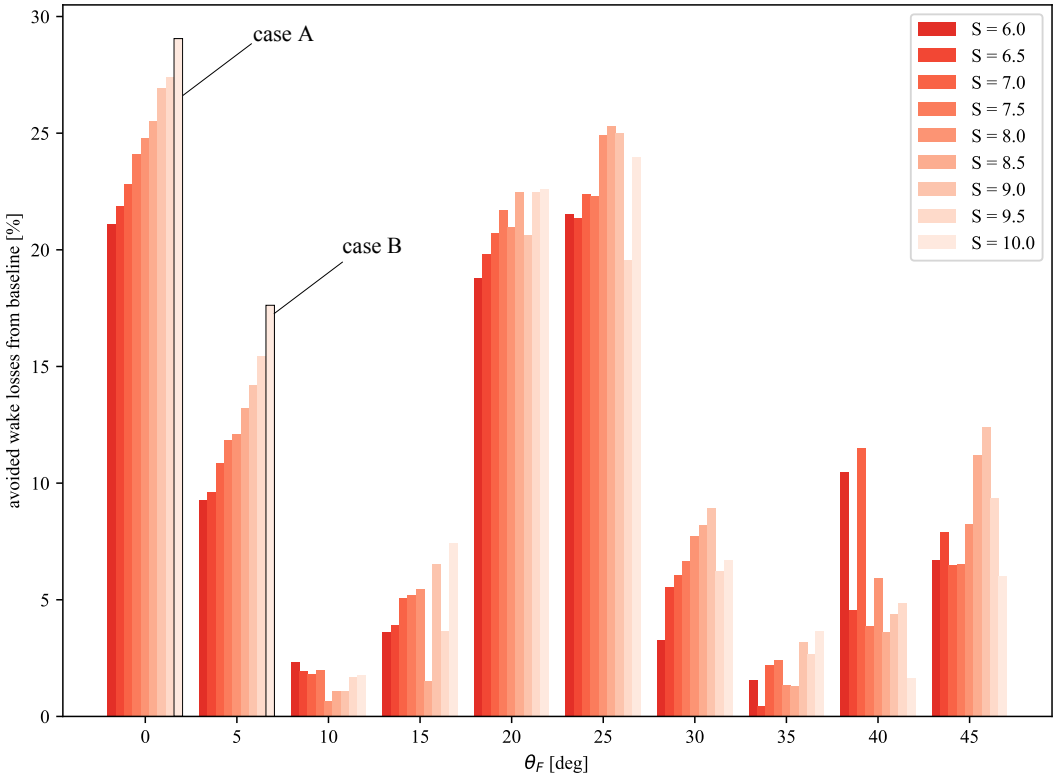

Figure 5. Comparison of wake loss reductions across farm-level variations in a square configuration relative to the baseline.

the wake effects. Minimal enhancement, with a mere 0.65% reduction in wake losses, is observed at $\theta_F = 10°$ and $S = 8.0$. In contrast, the maximum improvement, a significant 29.05% reduction in wake losses, is noted at $\theta_F = 0°$ and $S = 10.0$. Hence, TRTLE is a robust solution for sub-optimally configured farms, particularly in wake-dominant scenarios. For example, Table 2 illustrates the number of turbines and the wind farm capacity when the two layouts share the same wake loss percentage at farm orientations ($\theta_F = 0°, 20°,$ and $25°$). The baseline requires a spacing increase to 7.5 to achieve similar wake effects compared to the TRTLE-optimized layout with a spacing of $S = 6$ with higher turbine count. This implies the feasibility of denser turbine deployment within the same wind energy area and high farm capacity under a standard layout while keeping wake losses at minimum, thereby enhancing energy production. Amongst the two proposed mooring orientation methods depicted in Figure 4(b), the plane variation is selected 57% of the time. However, chessboard pattern has a higher potential for avoiding wake effects with an average of 20% compared to mere 6% for the plane variation method. This indicates that chessboard pattern is very effective for unfavorable farm properties that have high wake losses but not as effective when wake losses are originally low.

In scenarios where optimal layout selection is unfeasible, TRTLE methodology enables developers to attain heightened production under diverse constraints. Consider, for instance, a developer constrained by financial limitations aiming to minimize the number of turbines deployed. The two cases annotated in Figure 5 highlight these options which involve deploying 36 turbines, each spaced 10 rotor diameters apart, at a farm orientation of $\theta_F = 0°,$ and $5°$. Given the farm parameters, case A and B share the same design constraints that govern the

Table 2. turbine count (farm capacity [GW])

layout	$\theta_F = 0°$	$\theta_F = 20°$	$\theta_F = 25°$
TRTLE	100 (1.50)	107 (1.61)	107 (1.61)
baseline	64 (0.96)	68 (1.02)	67 (1.01)

ratio of anchor horizontal distance to water depth;

$$\frac{x_a}{d} = \frac{S \times D}{2d} = 1.211. \tag{3}$$

The adapted mooring configuration to the 2-line design at water depth of 1000m has the corresponding catenary coefficient β and mooring line length presented in Table 3. This ensures the platform motion is constrained to the maximum allowable excursion, e_{max}. The normalized watch circles for the baseline and the optimized mooring configuration adapted from moderate to deep water location are plotted in Figure 6. In addition to the baseline having smaller excursions, the mooring orientation of the baseline design (3-line) is considered identical for all wind turbines in the farm. This leads to similar offsets of all turbines and negligible effects on the wake computation.

Case A coincides with the most optimistic results and the optimum design for case B achieves a 17.62% reduction in wake effects. The TRTLE optimization technique selects the chessboard pattern for case A and plane variation pattern for case B. Figure 7(a) and Figure 8(a) detail TRTLE's mooring line configurations and anchor points, alongside the watch circle (rendered as an ellipse). Furthermore, in the event of mooring line failure, the affected turbine drifts towards the alternate anchor, remaining within a defined failure circle. This circle, where the turbine resides post-failure, assumes a mooring line with catenary shape $\beta = 1$ and $L_m = L_{m_{\max}}$, indicating the touchdown point directly beneath the fairlead. Since it is highly unlikely for two opposite mooring lines in two wind turbines fail at the same instant, line failure circles are allowed to overlap. However, they must not overlap with neighboring turbines' watch circles to mitigate collision risks. Figure 7(b) and Figure 8(b) delineate the wake patterns induced by prevailing wind in the baseline case, juxtaposed with the TRTLE wake. Notably, TRTLE's wake is broader, due to turbine repositioning, thereby augmenting overall farm energy output. Note that the possibility of mooring lines to share anchors is likely especially for case A with chessboard pattern mooring orientation. This is a topic for future studies.

Table 3. Example of mooring design adaptation to 1000m, 2-line mooring configuration under excursion and anchor radius constraints ($S = 10$).

$x_a/d = 1.211$	$e_{max}[m]$	$x_a[m]$	$\beta[-]$	$L_m[m]$	$\max(e/e_{max})[-]$	
					2-line	3-line
$d = 200m$	80	242.2	0.118	274.57	1.05	0.33
$d = 1000m$	400	1211.2	0.296	1701.35	1.01	0.25

4.2. Umbilical design and analysis

The TRTLE mooring configuration allows high horizontal excursions of the platform. This puts further constraints on the design of the power cable (umbilical). The umbilical faces

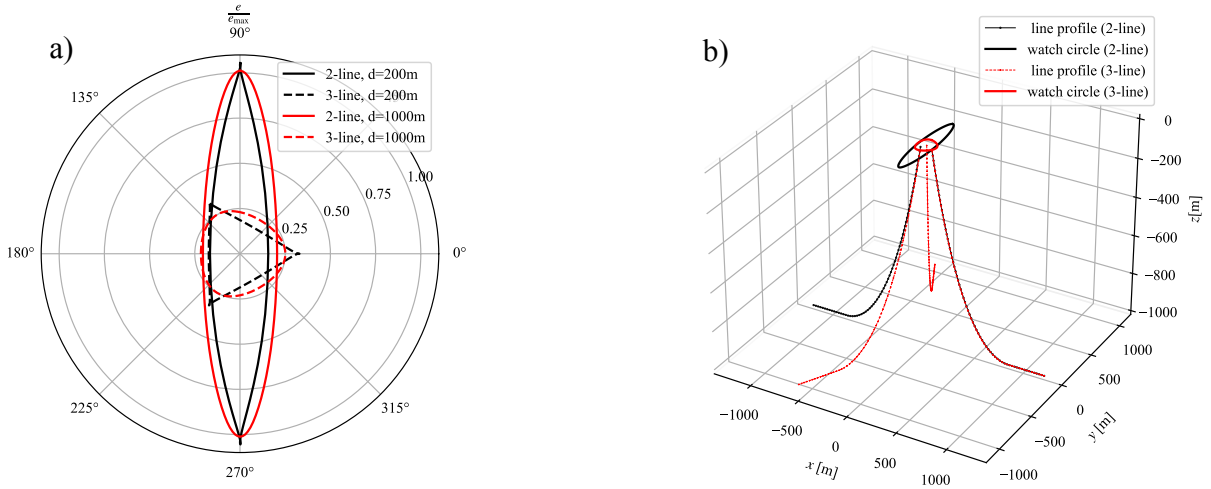

Figure 6. a) normalized watch circle of an optimized mooring design example of 2-line mooring configuration compared to the baseline 3-line mooring configuration at moderate and deep water depths for $S = 10$ and b) mooring lines profile for the 2-line and 3-line system.

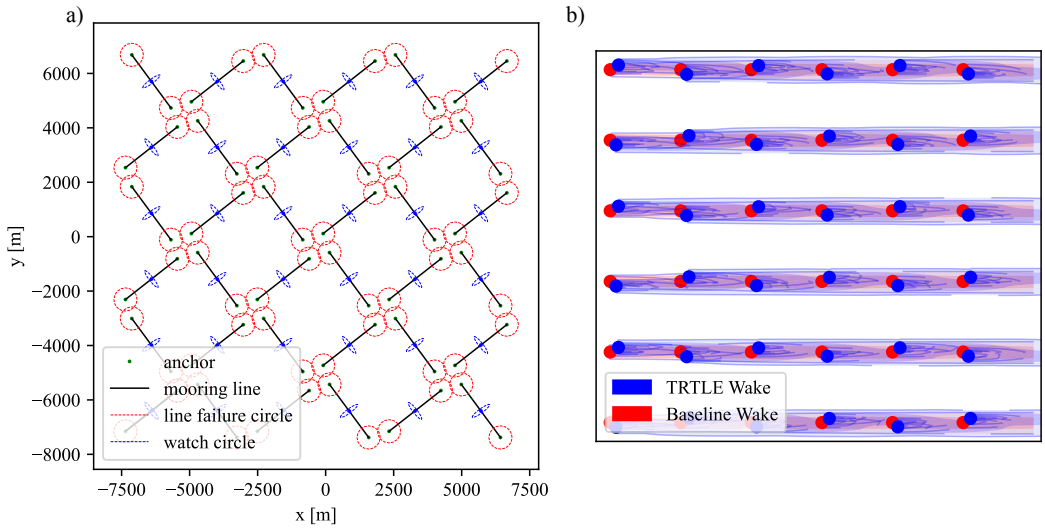

Figure 7. Case A: a) TRTLE farm-level configuration with visuals of anchor locations, mooring lines, watch circle, and line failure circle for the studied case of lowest number of turbines and b) wake visuals of baseline and TRTLE layered on top of each other for the prevailing wind direction from the west

highest variations in tensions and curvature if it is perpendicular to the 2-line mooring setup (i.e. the angle between ϕ_u and ϕ_m is a right angle). Therefore, to be conservative, all umbilical analysis and design assume maximum excursion and perpendicular configuration between the lines and the cable. Traditionally, the umbilical must be designed to prevent high tensions and high curvatures in the power cable while keeping it suspended in the water column under all conditions. Hence, two constraints are defined here:

- near constraint: when the platform offsets towards the umbilical cable, a clearance distance between the lowest point of the hang-off catenary section (the sag portion) and the seabed

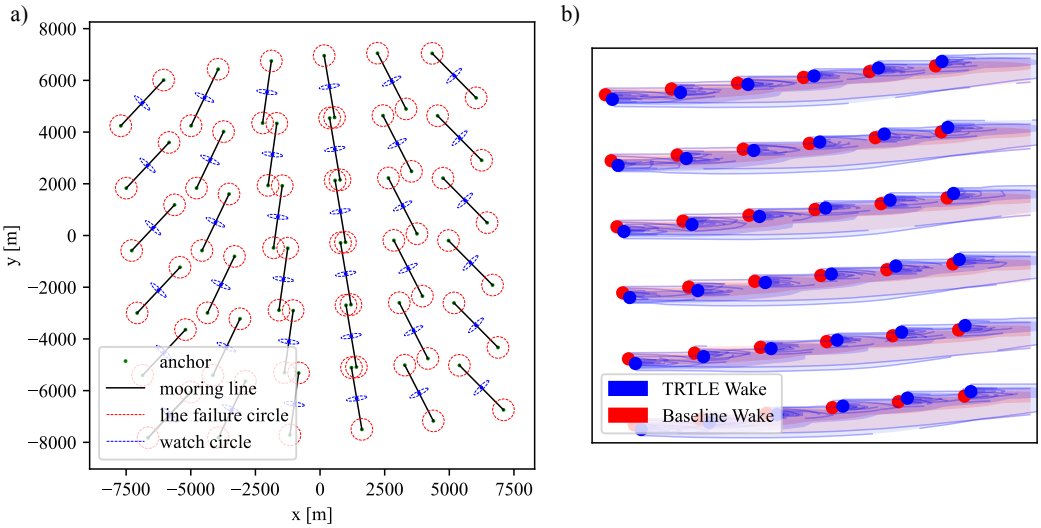

Figure 8. Case B: a) TRTLE farm-level configuration with visuals of anchor locations, mooring lines, watch circle, and line failure circle for the studied case of lowest number of turbines and b) wake visuals of baseline and TRTLE layered on top of each other for the prevailing wind direction from the west

must be kept higher than 10% of the water depth [20],

- far constraint: when the platform offsets away from the umbilical cable, maximum tension at the bend stiffener (the section where the umbilical and the platform meets) must be kept below than 20% the tension value of the nominal position (zero offset).

Two different configurations for the umbilical are chosen for this investigation: a single lazy-wave, and a double lazy-wave [32]. As the name suggests, the single lazy wave has one hang-off section, one buoyancy section, and one last touchdown catenary section. Whereas the double lazy-wave has two hang-off, two buoyancy, and one touchdown sections. The optimization problem investigates the variation of umbilical-related non-dimensional parameters that would satisfy the aforementioned constraints. These parameters are:

- the ratio of the total cable's length, L_u, to the umbilical horizontal reach, $(\frac{L_u}{x_u})$, varies between 0.75 and 2,
- the ratio of the umbilical horizontal reach to the water depth, $(\frac{x_u}{h})$, varies between 1.4 and 1.8,
- the ratio of the hang-off catenary section(s) length to the total cable length, $\frac{\ell_1}{L_u}$, varies between $0.5 < \frac{\ell_1}{L_u} < 0.8$ for a single lazy-wave and $0.15 < \frac{\ell_1}{L_u} < 0.3$ for double lazy-wave configuration, and
- the ratio of the buoyancy catenary section(s) length to the total cable's length, $\frac{\ell_2}{L_u}$, varies between $0.05 < \frac{\ell_2}{L_u} < 0.1$ for both configurations.

The bend stiffener is modelled as a steel section for the first 1m with 120e3 kN.m^2 bend stiffness and 5m as polymer section with a bending moment value of 103 kN.m under curvature of 1.12×10^{-3} rad/m. These values, as well as the umbilical cross-sectional properties, are replicated from the work of Ottesen [21]. This resulted in two configurations successfully able to meet the two constraints. Figure 9 compares the two solutions to one another at nominal, near, and far platform excursions. It is clear that the double-wave is more favorable in terms

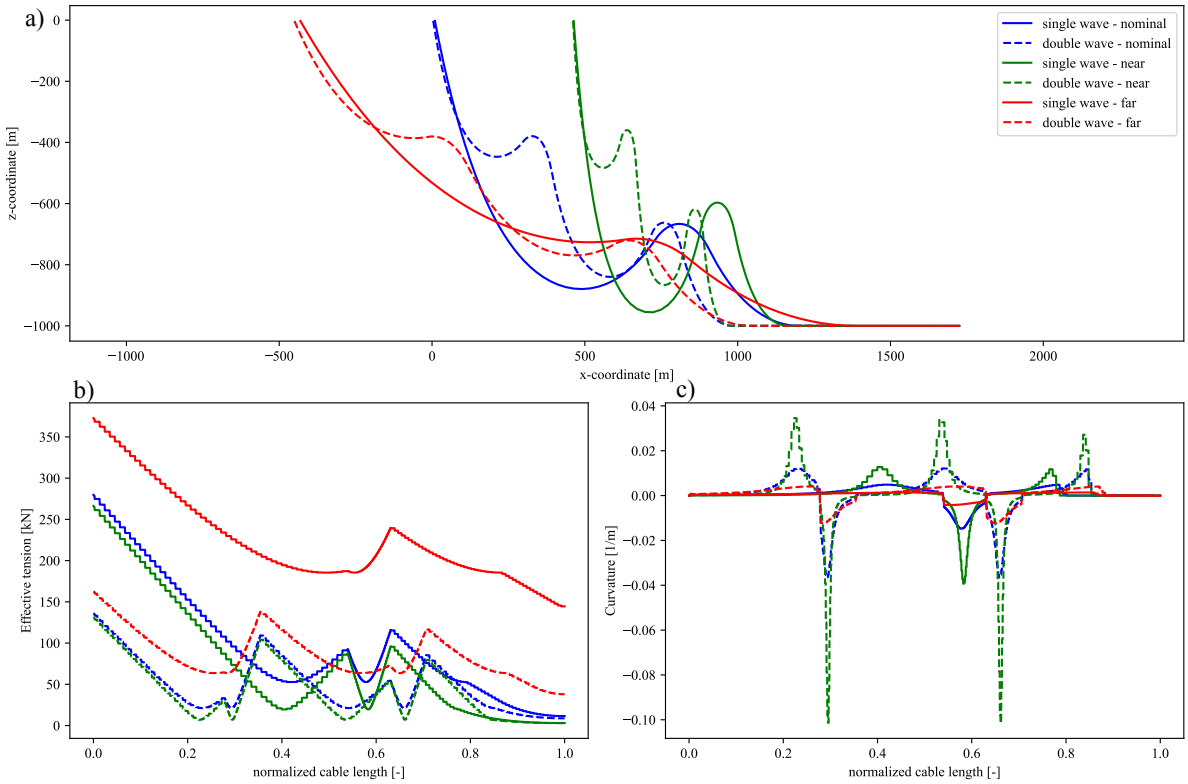

Figure 9. a) umbilical cable profiles, b) tensions, and c) curvatures in nominal, near, and far excursions

of seabed clearance (16% of water depth compared to 12% for a single lazy wave configuration) and lower tensions in the bend stiffener under far excursions (a little above 150 kN compared to over 350 kN). The double lazy-wave shows worse response than single lazy-wave in curvature as expected. These are static results and the dynamic excitation of the umbilical cable must be examined in future work, particularly at the bend stiffener.

5. Conclusions and remarks for future studies

This paper highlighted a new mooring conceptual design framework, TRTLE, that aims to minimize wake losses by considering their variation with respect to the turbines layout in the farm. It is shown that TRTLE is capable of limiting wake losses, hence advancing the energy yield of the farm when compared to the baseline cases where platforms' excursions are limited. The level of improvement depends on the level of optimality of the baseline layout. Developers can be faced with multitude of constraints that force them to select a sub-optimal layout as far as wake effects are concerned. These restrictions vary from increasing the farm production, which lead to higher number of turbines and higher wake losses, competing use of the sea for military, nature, or shipping routes, and others. TRTLE provides a solution to reducing wake effects by allowing each platform to relocate with limited excursion depending on the wind speed and direction while reducing mooring complexity and cost. Parametric analysis of farm-level parameters illustrated a reduction in wake effects between 1% and 30% when TRTLE is applied at rated wind speeds. The umbilical cable is redesigned and analyzed to allow for such excursions to take place without risking the cable touching the seabed in near excursions and avoiding high tensions in far excursions. The proposed double lazy-wave configuration accommodates higher

platform excursions at the expense of increased curvature in the hang-off and buoyancy sections.

For future research, exploring the impact of TRTLE on wake reduction in realistic wind farms, under realistic wind conditions, is crucial. For instance, the analysis presented here are limited of a single wind speed. This limitation overestimates both wake effects and annual energy yields as the farm produces less power in lower wind speeds and velocity deficit due to wake effects become irrelevant to the produced energy at high wind speeds. Furthermore, conducting dynamic analyses of the mooring configuration and power cable is critical to assess the soft mooring's low natural frequencies in horizontal motions, investigate possible resonance with environmental forces, and estimate the extreme excursions and line tensions. Additionally, it is imperative to investigate the economical aspects of the proposed solution. The proposed design is assumed to have multiple economical advantages in terms of increasing energy production, reducing wake effects and wake-induced fatigue loads on downstream turbines, reducing the number of mooring lines and anchors usually required to limit horizontal excursions, and reducing tension-induced fatigue on the mooring systems due to its relaxed configuration. On the other hand, it might have implications that might increase the overall cost such as those driven by designing specialized mooring and umbilical cables and additional cost to introduce more redundancy to the system. For instance, the umbilical might need to be increased in length, which might increase the footprint on the seabed. Due to high excursions, the laid portion of the mooring line on the seabed can cause more disturbances, which in turn can disturb aquatic life in its proximity. These issues must be addressed in future work.

6. Acknowledgment

The authors would like to acknowledge the support from the Norwegian Directorate for Higher Education and Skills (HK-dir) through the NUWind Project (Project number UTF-2021/10157).

References

[1] Campanile, A., Piscopo, V. and Scamardella, A., 2018. Mooring design and selection for floating offshore wind turbines on intermediate and deep water depths. Ocean Engineering, 148, pp.349-360.
[2] Lee J and Zhao F 2022 *Global wind report 2022*. `https://gwec.net/global-wind-report-2022/`
[3] González, J.S., Payán, M.B., Santos, J.M.R. and González-Longatt, F., 2014. A review and recent developments in the optimal wind-turbine micro-siting problem. Renewable and Sustainable Energy Reviews, 30, pp.133-144.
[4] Neubert, A., Shah, A. and Schlez, W., 2010, November. Maximum yield from symmetrical wind farm layouts. In Proceedings of DEWEK (Vol. 98).
[5] *Uniform turbine layout touted for NE US offshore wind*, Accessed 2 January 2020; 2019 `https://renews.biz/56505/`
[6] Gonzalez-Rodriguez, A.G., Serrano-Gonzalez, J., Burgos-Payan, M. and Riquelme-Santos, J., 2022. Multi-objective optimization of a uniformly distributed offshore wind farm considering both economic factors and visual impact. Sustainable Energy Technologies and Assessments, 52, p.102148.
[7] Kheirabadi, A.C. and Nagamune, R., 2019. A quantitative review of wind farm control with the objective of wind farm power maximization. Journal of Wind Engineering and Industrial Aerodynamics, 192, pp.45-73.
[8] Jiménez, Á., Crespo, A. and Migoya, E., 2010. Application of a LES technique to characterize the wake deflection of a wind turbine in yaw. Wind energy, 13(6), pp.559-572.
[9] Equinor 2022 *Floating Wind*
[10] Kheirabadi, A.C. and Nagamune, R., 2020. Real-time relocation of floating offshore wind turbine platforms for wind farm efficiency maximization: An assessment of feasibility and steady-state potential. Ocean Engineering, 208, p.107445.
[11] Kheirabadi, A.C. and Nagamune, R., 2019, July. Modeling and power optimization of floating offshore wind farms with yaw and induction-based turbine repositioning. In 2019 American Control Conference (ACC) (pp. 5458-5463). IEEE.
[12] Han, C., Homer, J.R. and Nagamune, R., 2017, May. Movable range and position control of an offshore wind turbine with a semi-submersible floating platform. In 2017 American Control Conference (ACC) (pp. 1389-1394). IEEE.
[13] Fleming, P., Gebraad, P.M., Lee, S., van Wingerden, J.W., Johnson, K., Churchfield, M., Michalakes, J.,

Spalart, P. and Moriarty, P., 2015. Simulation comparison of wake mitigation control strategies for a two-turbine case. Wind Energy, 18(12), pp.2135-2143.
[14] Ceriello, V., 2023. Wake Effect Mitigation of Floating Offshore Wind Farms: Combining Layout Optimization, Turbine Repositioning and Yaw-based Wake Redirection. TUDelft Master's thesis.
[15] Kilinç, U., 2022. Dynamic wind farm layout optimization: To find the optimal spots for movable floating offshore wind turbines through dynamic repositioning.
[16] Rodrigues, S.F., Pinto, R.T., Soleimanzadeh, M., Bosman, P.A. and Bauer, P., 2015. Wake losses optimization of offshore wind farms with moveable floating wind turbines. Energy conversion and management, 89, pp.933-941.
[17] Mahfouz, M.Y. and Cheng, P.W., 2023. A passively self-adjusting floating wind farm layout to increase the annual energy production. Wind Energy, 26(3), pp.251-265.
[18] Mahfouz, M.Y., Hall, M. and Cheng, P.W., 2022, May. A parametric study of the mooring system design parameters to reduce wake losses in a floating wind farm. In Journal of Physics: Conference Series (Vol. 2265, No. 4, p. 042004). IOP Publishing.
[19] Schnepf, A., Lopez-Pavon, C., Devulder, A., Johnsen, Ø. and Ong, M.C., 2022, June. Suspended power cable configurations for floating offshore wind turbines in deep water powering an FPSO. In International Conference on Offshore Mechanics and Arctic Engineering (Vol. 85932, p. V008T09A049). American Society of Mechanical Engineers.
[20] Rentschler, M.U., Adam, F. and Chainho, P., 2019. Design optimization of dynamic inter-array cable systems for floating offshore wind turbines. Renewable and Sustainable Energy Reviews, 111, pp.622-635.
[21] Ottesen, T., 2010. Extreme response estimation of umbilical on very deep water (Master's thesis, Norges teknisk-naturvitenskapelige universitet, Fakultet for ingeniørvitenskap og teknologi, Institutt for marin teknikk).
[22] Allen, C., Viscelli, A., Dagher, H., Goupee, A., Gaertner, E., Abbas, N., Hall, M. and Barter, G., 2020. Definition of the UMaine VolturnUS-S reference platform developed for the IEA wind 15-megawatt offshore reference wind turbine (No. NREL/TP-5000-76773). National Renewable Energy Lab.(NREL), Golden, CO (United States); Univ. of Maine, Orono, ME (United States).
[23] Gaertner, E., Rinker, J., Sethuraman, L., Zahle, F., Anderson, B., Barter, G.E., Abbas, N.J., Meng, F., Bortolotti, P., Skrzypinski, W. and Scott, G.N., 2020. IEA wind TCP task 37: definition of the IEA 15-megawatt offshore reference wind turbine (No. NREL/TP-5000-75698). National Renewable Energy Lab.(NREL), Golden, CO (United States).
[24] NREL. FLORIS. Version 2.4, 2021. Available online: `https://github.com/nrel/floris`
[25] Katic, I., Højstrup, J. and Jensen, N.O., 1986, October. A simple model for cluster efficiency. In European wind energy association conference and exhibition (Vol. 1, pp. 407-410). Rome, Italy: A. Raguzzi.
[26] van Binsbergen, D., Daems, P.J., Verstraeten, T., Nejad, A. and Helsen, J., 2023. Hyperparameter tuning framework for calibrating analytical wake models using SCADA data of an offshore wind farm applied on FLORIS. Wind Energy Science Discussions, 2023, pp.1-28.
[27] Baker, N.F., Stanley, A.P., Thomas, J.J., Ning, A. and Dykes, K., 2019. Best practices for wake model and optimization algorithm selection in wind farm layout optimization. In AIAA Scitech 2019 forum (p. 0540).
[28] Optuna: A hyperparameter optimization framework. Available online: `https://optuna.readthedocs.io/en/stable/index.html`
[29] Watanabe, S., 2023. Tree-structured Parzen estimator: Understanding its algorithm components and their roles for better empirical performance. arXiv preprint arXiv:2304.11127.
[30] Campanile, A., Piscopo, V. and Scamardella, A., 2018. Mooring design and selection for floating offshore wind turbines on intermediate and deep water depths. Ocean Engineering, 148, pp.349-360.
[31] Brommundt, M., Krause, L., Merz, K. and Muskulus, M., 2012. Mooring system optimization for floating wind turbines using frequency domain analysis. Energy Procedia, 24, pp.289-296.
[32] Zhao, S., Cheng, Y., Chen, P., Nie, Y. and Fan, K., 2021. A comparison of two dynamic power cable configurations for a floating offshore wind turbine in shallow water. AIP Advances, 11(3).